J Water Environ Nanotechnol 2026, 11(1): 67-83
10.22090/jwent.2026.01.06

Supporting Information

For

Novel highly efficient adsorbent material based on MIL-101 MOF doped with Mn for Cu(II) decontamination from wastewater

Sheta Mohamed Sheta1*, Eman A. Elmenofy2, Omnia I. Ali2, A. T. Kandil2, Said M. El-sheikh 3

1 Inorganic Chemistry Department, National Research Centre, 33 El-Behouth St., Dokki, Giza, Egypt.
2 Department of Chemistry, Faculty of Science, Helwan University, Cairo, Egypt.
3 Department of Nanomaterials and Nanotechnology, Central Metallurgical R & D Institute, Cairo, Egypt.

* Corresponding Author.
Sheta M. Sheta
Email: dr.sheta.nrc@gmail.com

Article History:
Received: 2025-06-25
Revised: 2025-09-18
Accepted: 2025-10-21

How to cite this article

Sheta SM, Elmenofy EA, Ali OI, Kandil AT, El-sheikh SM. Novel highly efficient adsorbent material based on MIL-101 MOF doped with Mn for Cu(II) decontamination from wastewater. J Water Environ Nanotechnol 2026, 11(1): 67-83, DOI: 10.22090/jwent.2026.01.06

HIGHLIGHTS

- A novel promising MIL-101-MOF doped with Mn was synthesized and fully characterized.
- MIL-101/0.5Mn MOF was used as a potential adsorbent substance for removal of Cu^{2+}.
- MIL-101/0.5Mn MOF showed higher R.E % in comparison to other sorbents.
- Excellent removal performance of MIL-101/0.5Mn MOF for Cu^{2+} from real active waste.
- Adsorption/thermodynamic studies, sorption isotherms and kinetics, were evaluated.

ABSTRACT

Although copper is classified as a heavy metal and is widely used across various industrial sector, it is also well-known for having detrimental effects on human health and the environment. In this work, manganese was used to produce and dope chromium terephthalate MOF (MIL-101(Cr)) using different molar ratios to create effective adsorbents: MIL-101/0.25Mn and MIL-101/0.5Mn MOFs. The MIL-101/0.5Mn MOF was specifically employed to remove Cu^{2+} ions from water and wastewater. The prepared samples were analyzed using XRD, SEM/EDX, TEM, FT-IR, TGA, XPS, and BET analysis. The doped MIL-101/0.5Mn crystals displayed a hexagonal crystal shape. The specific surface areas of the synthesized MIL-101 and MIL-101/0.5Mn MOFs were high, measuring 1009.53 and 1676.59 m^2 g^{-1}, respectively, and exhibited characteristics of a mesoporous structure. The MIL-101/0.5Mn MOF displayed a high capacity for Cu^{2+} adsorption of 124.97 mg g^{-1} and, even after five cycles, maintained a strong removal ability. Endothermic and spontaneous Cu^{2+} adsorption occurred on the MIL-101/0.5Mn MOF, with equilibrium findings indicating a good fit to pseudo-second-order kinetics and Langmuir isotherm studies. The MIL-101/0.5Mn MOF demonstrated better copper removal efficacy relative to other studies. The results suggested copper (II) was adsorbed by surface complexation and electrostatic attraction. Furthermore, the Cu^{2+} recovery from water samples ranged between 89.1% and 95.8%, indicating the remarkable efficiency of the MIL-101/0.5Mn MOF for copper removal from real samples.

KEYWORDS: MIL-101-MOF; Wastewater; Cu(II) decontamination; Adsorption; Thermodynamic

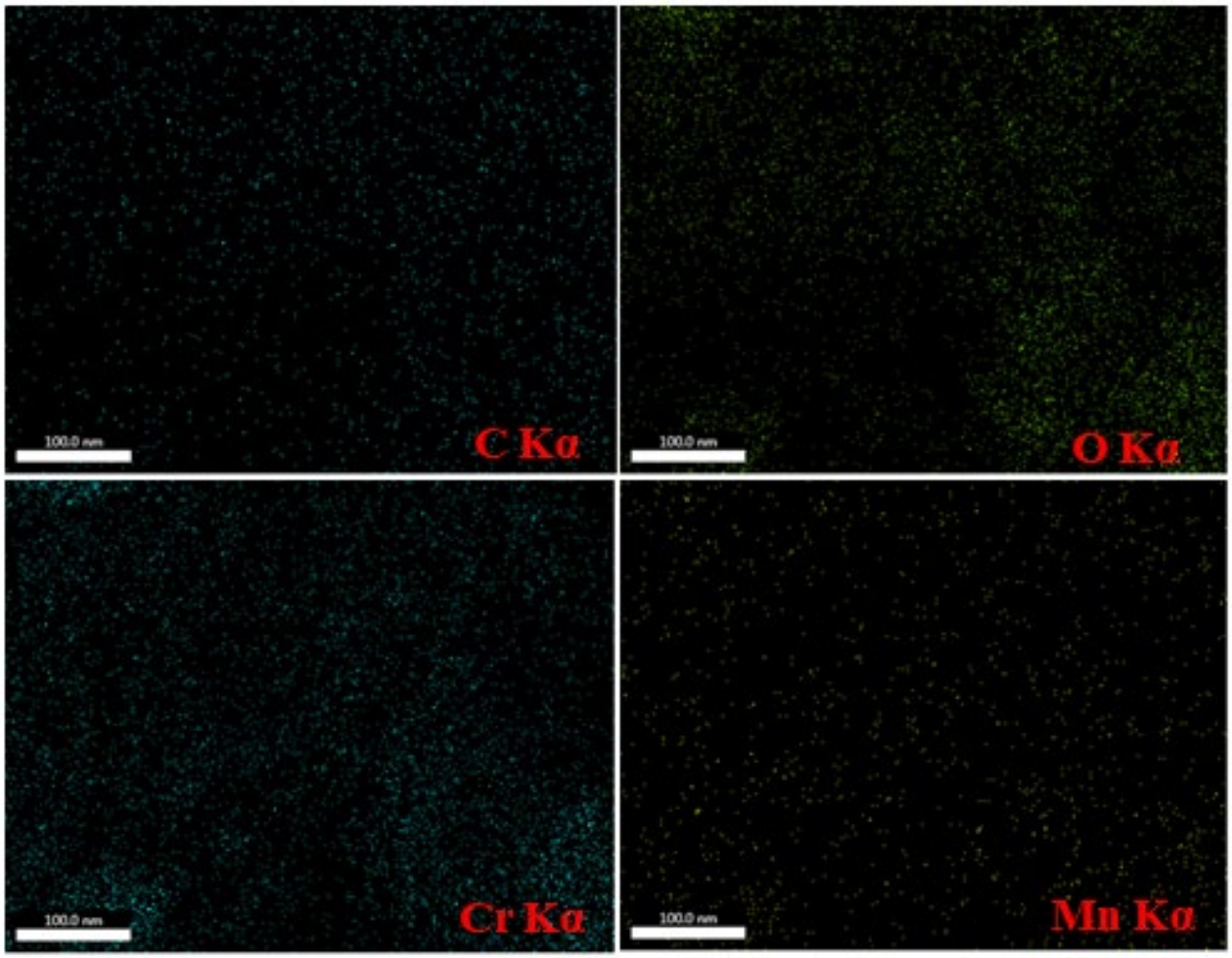

Fig. S1. Elemental mapping of C, O, Cr, and Mn for MIL-101/0.5Mn MOF.

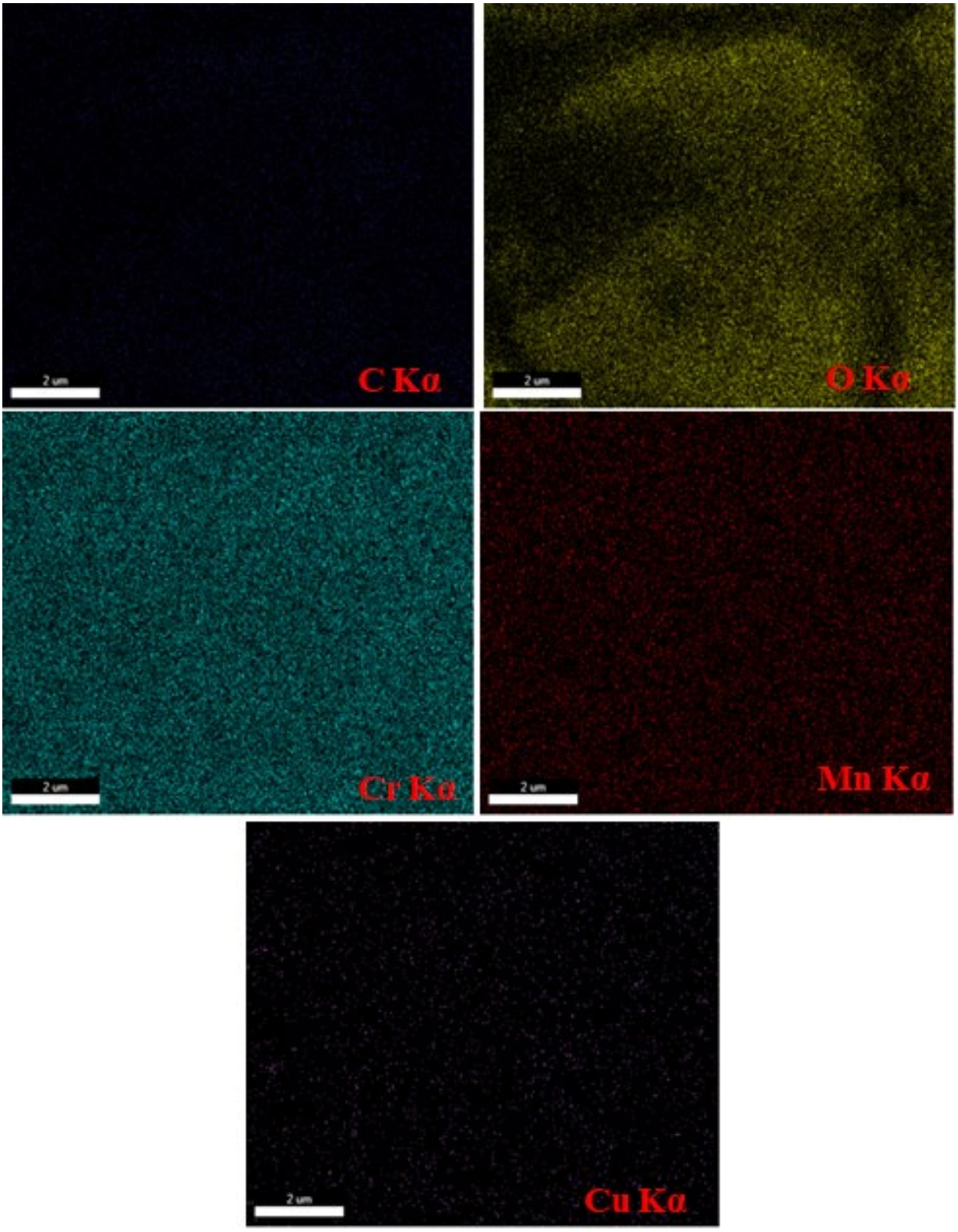

Fig. S2. Elemental mapping of C, O, Cr, Mn, and Cu for MIL-101/0.5Mn MOF after Cu^{2+} adsorption.

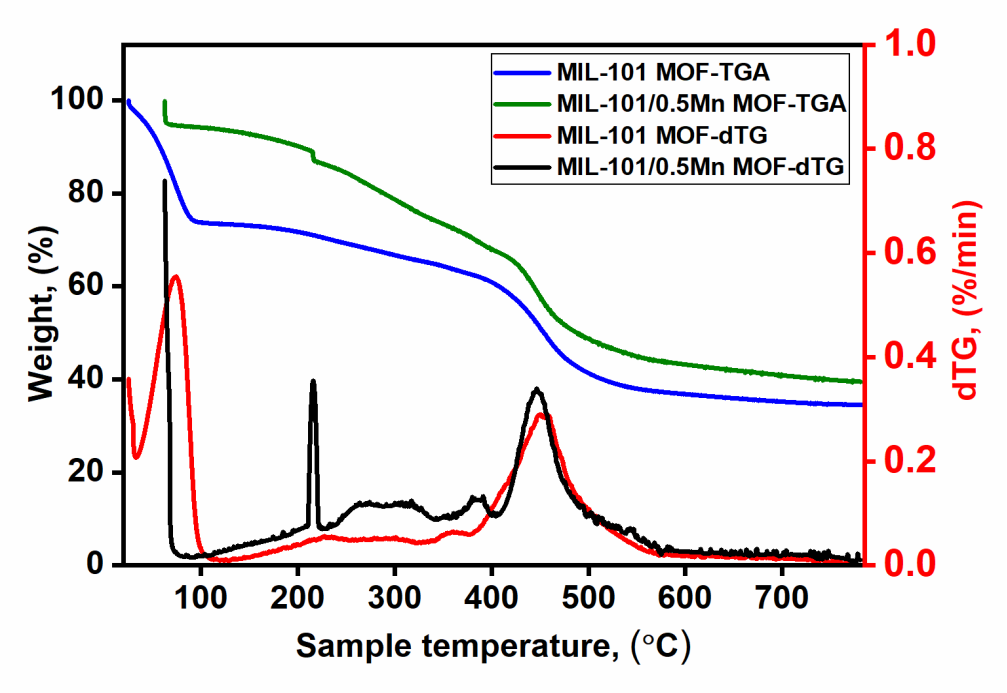

Fig. S3. TGA analysis of MIL-101 and MIL-101/0.5Mn MOFs.

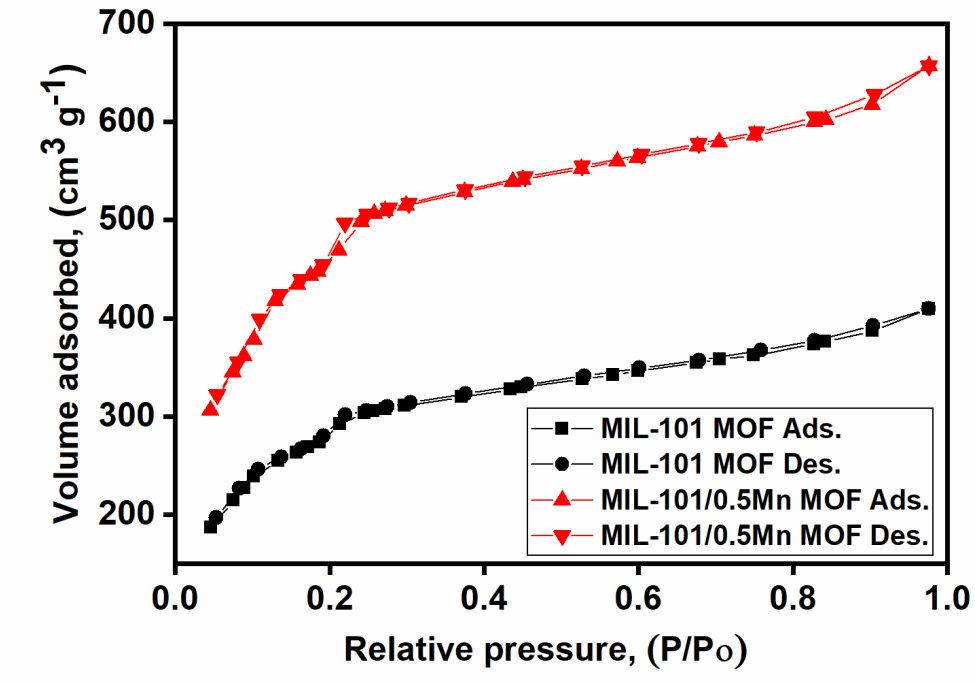

Fig. S4. BET analysis of MIL-101 and MIL-101/0.5Mn MOFs.

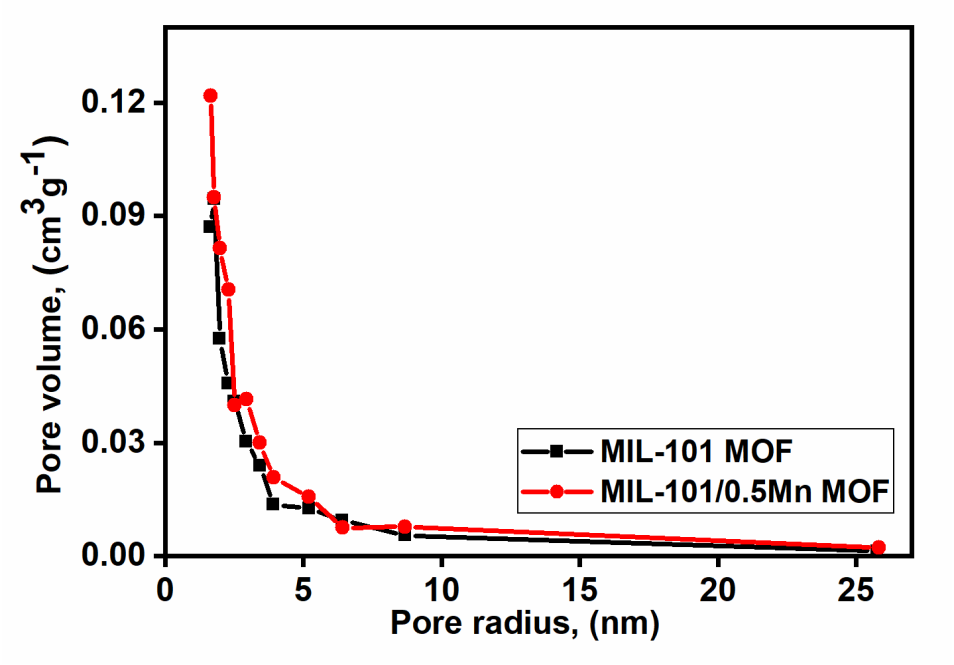

Fig. S5. Pore size distribution of MIL-101 and MIL-101/0.5Mn MOFs.

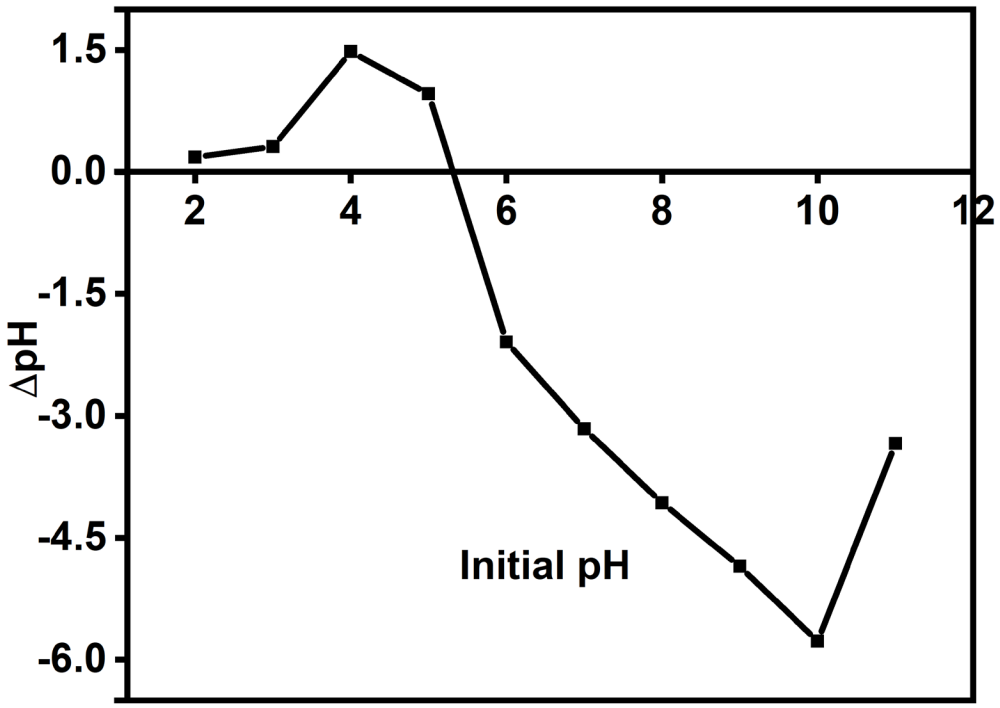

Fig. S6. pH_{pzc} of MIL-101/0.5Mn MOF.

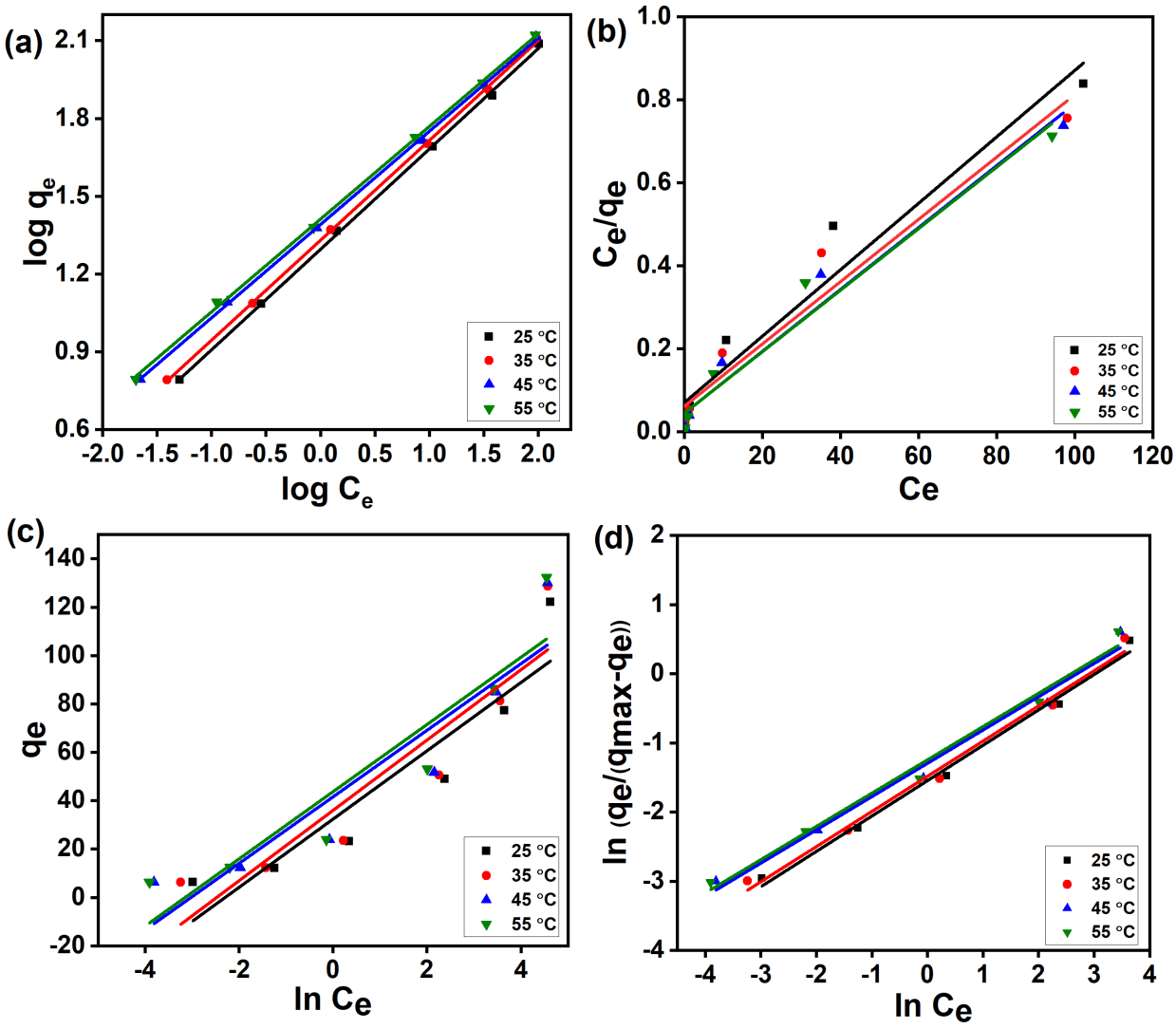

Fig. S7. Adsorption isotherms' plots for Cu^{2+} removal at different temperatures using MIL-101/ 0.5Mn MOF: **(a)** Freundlich, **(b)** Langmuir, **(c)** Temkin, and **(d)** Sips.

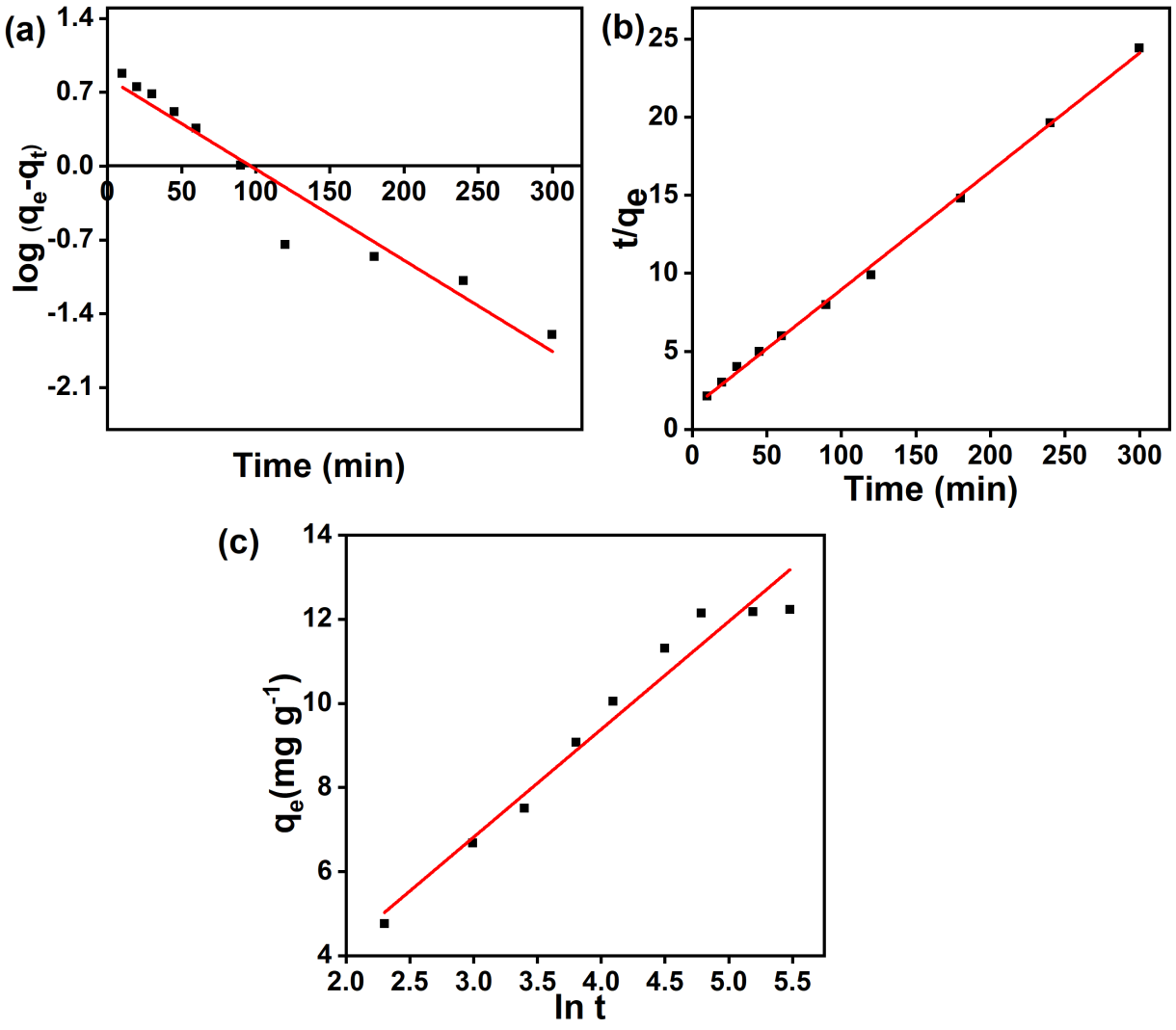

Fig. S8. Kinetics' plots for Cu^{2+} removal using MIL-101/0.5Mn MOF: **(a)** pseudo-first order; **(b)** pseudo-second order; and **(c)** Elovich kinetics models.

Table S1. Physicochemical characteristics of the employed real water samples.

Test	Tap water	Groundwater	Industrial water
Total alkalinity, mg/L	140	148.72	130
Turbidity, NTU	0.5	---	11.90
pH	7.3	7.82	7.51
Temperature, °C	25	25	25
EC, µS/cm	400	393	437
T.D.S., mg/L	264	288.84	281
Total Hardness, mg/L	142	76.6	131
Ca hardness, mg/L	72	45.68	79
Mg hardness, mg/L	70	30.92	52
Cl, mg/L	23	26.88	28.40
F, mg/L	0.3	---	0.4
Na, mg/L	14	23.16	---
K, mg/L	20	6.92	---
SO_4, mg/L	40	44.76	---
SiO_2, mg/L	3	---	5.6
NO_3, mg/L	2 mg/L	---	Nil
NH_4, mg/L	Nill	---	---
NO_2, mg/L	Nill	---	---
		Fe^{3+}: 0.045	Fe^{3+}: 0.008
		Ni: 0.1664	Zn: 0.168
		Co < 0.01	Co < 0.01
		Pb < 6.5	Pb < 0.03
		Cd < 0.001	Cd < 0.001
		Mn < 0.4	Mn < 0.01
		Hg < 0.001	Hg < 0.001

S1. Instruments

The X-ray diffraction patterns of samples were achieved on a D8 advance X-ray diffractometer (Bruker AXS D8, Karlsruhe, Germany) that was set up with Cu-Kα radiation (λ = 0.154056 nm) to identify the crystalline phase of the prepared samples in the range of 2θ from 5° to 70°. N_2 adsorption–desorption isotherms at 77 K and the samples' porosity were determined using Quantachrome TouchWin™ (version 1.2, USA). The Fourier transform infrared (FT-IR) spectra of MOFs were recorded with a Perkin Elmer FT/IR-109979 spectrophotometer (JASCU, USA) with the use of KBr tablets in the range from 400 to 4000 cm^{-1}. Thermogravimetric analysis (TGA) and differential thermal analysis (DTA) of MIL-101 and MIL-101/0.5Mn MOFs were studied with Universal V4.5-TA Instruments (USA). The test conditions were set as follows: argon flow at 30 mL min^{-1} and a heating rate of 10°C min^{-1} across a temperature range of 30–800°C. SEM images and EDX spectra of MIL-101 and MIL-101/0.5Mn (before and after copper adsorption) MOFs were recorded with a combination of field emission scanning electron microscopy (FE-SEM) and energy-dispersive X-ray spectroscopy (EDX) (JEOL JSM-6510LV, Japan). The morphology of MIL-101/0.5Mn MOF was examined by using a high-resolution transmission electron microscope (HR-TEM) with an acceleration voltage up to 200 kV (JEM-2100-JEOL, Japan). The oxidation states and species of the MIL-101/0.5Mn MOF were recorded by the Thermo Scientific™ K-Alpha™ X-ray photoelectron spectrometer (XPS) (Thermo Scientific, USA), using Al-Kα micro-focused monochromator within an energy range up to 4 keV. Copper concentration was analyzed using a UV-Vis spectrophotometer model 630 V (Jasco, Japan).

S2. Adsorption Experiments

In order to do sorption studies in batch mode, 0.02 g of Mn-doped MIL-101 was combined with a solution of copper of 25 mL (10 mg L^{-1}) and the solutions were constantly shaking at 180 rpm. And, to alter the pH of the aqueous solutions, NaOH and HCl (0.1 mol L^{-1}) were added. For two hours, the batch tests were conducted at ambient temperature. Following adsorption, the adsorbent was removed by filtering, and DDTC was used to perform the spectrophotometric analysis of the concentration of residual Cu^{2+} ions (Elmenofy et al. 2025).

The removal percentage and the amount of heavy metal adsorbed were calculated using Eqs. S1 and S2:

$$\text{Removal } \% = \frac{(C_i - C_e)}{C_i} * 100 \quad \text{(S1)}$$

$$q_e = (C_i - C_e)\, V/m \quad \text{(S2)}$$

where V is the initial solution's volume (L), q_e represents the quantity of heavy metal adsorbed onto the Mn-doped MIL-101 (mg g^{-1}), the concentrations at the start and finish of a period, represented as C_i and C_e are those (mg L^{-1}), and m is Mn-doped MIL-101's mass (g).

S3. Adsorption Isotherms

The Cu^{2+} adsorption process using MIL-101/0.5Mn MOF was fitted by four isotherm models of Langmuir, Freundlich, Temkin, and Sips isotherms. The *Langmuir* isotherm assumes monolayer adsorption on a uniform surface with a finite number of adsorption sites. Once a site is filled, no further adsorption can take place at that site. The linear form of the Langmuir isotherm model is described as:

$$\frac{C_e}{q_e} = \frac{1}{K_L\, q_{max}} + \frac{C_e}{q_{max}} \quad \text{(S3)}$$

where K_L is the Langmuir constant related to the energy of adsorption and q_{max} is the maximum adsorption capacity (mg g^{-1}).

The favorability and feasibility of adsorption process of Cu^{2+} using MIL-101/0.5Mn MOF can be determined by the separation factor (R_L) in the analysis of data by Langmuir isotherm. It is given by the following Eq.

$$R_L = \frac{1}{1 + K_L C_i} \quad \text{(S4)}$$

The value of R_L indicates the type of isotherm as follows: unfavorable ($R_L > 1$), linear ($R_L = 1$), favorable ($0 < R_L < 1$) or reversible ($R_L = 0$).

The *Freundlich* isotherm is applicable to both monolayer (chemisorption) and multilayer adsorption (physisorption) and assumes that the adsorbate adsorbs onto the heterogeneous surface of an adsorbent. The linear form of Freundlich equation is expressed as:

$$\log q_e = \frac{1}{n} \log C_e + \log K_F \quad \text{(S5)}$$

where K_F and n are Freundlich isotherm constants related to adsorption capacity and adsorption intensity, respectively.

The *Temkin* isotherm model assumes that the adsorption energy decreases linearly with the surface coverage due to adsorbent–adsorbate interactions. The linear form of Temkin isotherm model is given by the equation:

$$q_e = RT \frac{\ln K_T}{b} + RT \frac{\ln C_e}{b} \quad \text{(S6)}$$

where K_T is the Temkin isotherm constant (L g^{-1}), b is the Temkin constant related to the heat of sorption (J mol^{-1}), and $R_T/b = B$.

The *Sips* isotherm is a combined form of Langmuir and Freundlich models deduced for predicting the adsorption in heterogeneous systems and avoiding the limitation of the rising adsorbate concentration associated with the Freundlich isotherm. At low adsorbate concentrations it reduces to the Freundlich isotherm, whereas at high concentrations it predicts monolayer adsorption in a similar manner as the Langmuir isotherm. Therefore, the Sips isotherm shall be used to describe only monolayer adsorption systems (Tzabar and ter Brake 2016).

$$\ln\left(\frac{q_e}{q_{max} - q_e}\right) = \frac{1}{n} \ln C_e + \ln K_s \quad \text{(S7)}$$

where K_S is the empirical constant of the Sips equation related to energy of adsorption (L/mg), and n is the adsorption intensity (Almeida-naranjo et al. 2021).

S4. Adsorption Kinetics

The respective experimental data at various contact times corresponding to changes in removal percentage were investigated using different kinetic models, including pseudo-first-order, pseudo-second-order, Weber-Morris intraparticle diffusion, and Elovich models.

The pseudo-first-order model is linearly expressed as:

$$\ln (q_e - q_t) = \ln q_e - k_1 t \quad \text{(S8)}$$

The pseudo-second order kinetic model is given as:

$$\frac{t}{q_t} = \frac{1}{k_2 {q_e}^2} + \frac{t}{q_e} \quad \text{(S9)}$$

Intraparticle diffusion model is linearly expressed as:

$$q_t = k_3 t^{0.5} + C \quad \text{(S10)}$$

Elovich model is represented by the following expression.

$$q_t = \frac{1}{\alpha} \ln \alpha\beta + \frac{1}{\alpha} \ln t \quad \text{(S11)}$$

where q_t and q_e are the amount of chromium ions adsorbed per unit of adsorbent (mg g^{-1}) at time t (min) and equilibrium respectively, k_1 is the pseudo first order rate constant (min^{-1}), k_2 is pseudo second order rate constant (g mg^{-1} min), k_3 is the intraparticle diffusion rate constant (mg g^{-1} $min^{1/2}$), C is the width of the limit layer, α is initial adsorbate adsorption rate (mg g^{-1} min^{-1}), and β is adsorption constant (mg g^{-1} min^{-1}).

S5. Adsorption Thermodynamics

For adsorption studies, thermodynamic investigations are necessary to specify the removal process's feasibility and spontaneity. Thus, considering the thermodynamic parameters in Eq. S12, such as the change in enthalpy (ΔH^o) and the change in entropy (ΔS^o) were computed based on experimental data from adsorption processes.

$$\ln K_S = \frac{\Delta S^\circ}{R} - \frac{\Delta H^\circ}{RT} \quad \text{(S12)}$$

where the K_S value was calculated using the Sips model equation (Lima et al. 2019). The plot of ln K_S versus 1/T was utilized to estimate the values of ΔH° and ΔS° based on their slope and intercept. Furthermore, Eq. S13 was used to estimate ΔG°, the Gibbs free energy change:

$$\Delta G^\circ = \Delta H^\circ - T\Delta S^\circ \quad \text{(S13)}$$

S6. Application

The analytical applicability of the suggested MIL-101/0.5Mn adsorbent for Cu^{2+} removal from several kinds of real water samples was investigated. Tap water, groundwater, and industrial water were among the samples employed.

References

Almeida-naranjo, Cristina E., María Belén, Génesis Cabrera, and Victor H. Guerrero. 2021. "Caffeine Removal from Synthetic Wastewater Using Magnetic Fruit Peel Composites : Material Characterization , Isotherm and Kinetic Studies Caffeine Removal from Synthetic Wastewater Using Magnetic Fruit Peel Composites : Material Characterization , Isothe." *Environmental Challenges* 5(November):100343. doi: 10.1016/j.envc.2021.100343.

Elmenofy, Eman A., Omnia I. Ali, A. T. Kandil, Sheta M. Sheta, and Said M. El-sheikh. 2025. "A Novel Ternary Composite of GO/NiCoFe 2 O 4 /MIL-53 for Enhanced Copper Removal from Wastewater." *European Journal of Inorganic Chemistry*. doi: 10.1002/ejic.202400795.

Lima, Eder C., Ahmad Hosseini-Bandegharaei, Juan Carlos Moreno-Piraján, and Ioannis Anastopoulos. 2019. "A Critical Review of the Estimation of the Thermodynamic Parameters on Adsorption Equilibria. Wrong Use of Equilibrium Constant in the Van't Hoof Equation for Calculation of Thermodynamic Parameters of Adsorption." *Journal of Molecular Liquids* 273:425–34. doi: 10.1016/j.molliq.2018.10.048.

Tzabar, Nir, and H. J. M. ter Brake. 2016. "Adsorption Isotherms and Sips Models of Nitrogen, Methane, Ethane, and Propane on Commercial Activated Carbons and Polyvinylidene Chloride." *Adsorption* 22(7):901–14. doi: 10.1007/s10450-016-9794-9.